Supplementary Material

Ubpy Controls the Stability of the ESCRT-0 Subunit Hrs in Development

Junzheng Zhang[1,2], Juan Du[1,2], Cong Lei[1], Min Liu[1,2] and Alan Jian Zhu[1,2,3]

[1] State Key Laboratory of Biomembrane & Membrane Biotechnology, Ministry of Education Key Laboratory of Cell Proliferation and Differentiation, Peking-Tsinghua Center for Life Sciences, College of Life Sciences, Peking University, Beijing 100871, China.

[2] Department of Cellular & Molecular Medicine, Lerner Research Institute, Cleveland Clinic, Cleveland, OH 44195, USA

[3] Author for correspondence (zhua@pku.edu.cn)

Table S1. Genotypes and cross conditions used in this study

Figure(s)	**Cross(es)**
Fig. 1A-P, Fig. 2Q-X, Fig. 3A, Fig. S2A-I, Fig. S4F	*hs-flp*;; FRT82B, *ubi-gfp* × FRT82B, $Ubpy^{KO}$ / TM6B
Fig. 1Q-T	*hs-flp*;; *ptc-lacZ* / +; FRT82B, *ubi-gfp* / + × FRT82B, $Ubpy^{KO}$ / TM6B
Fig. 1U-X	*hs-flp*;; *dpp-lacZ* / +; FRT82B, *ubi-gfp* / + × FRT82B, $Ubpy^{KO}$ / TM6B
Fig. 2A-P, Fig. 3B,C, Fig. S4A-E, Fig. S8G-H	*hs-flp*;; FRT82B, *arm-lacZ* × FRT82B, $Ubpy^{KO}$ / TM6B
Fig. 3D,D'	*ubi-gfp, hs-flp,* FRT19A × dor^{8}, FRT19A / FM7
Fig. 3E,E'	*hs-flp*;; FRT82B, *ubi-gfp* × FRT82B, $vps22^{ZZ13}$ / TM6B
Fig. 3F,F'	*hs-flp*;; FRT82B, *ubi-gfp* × FRT82B, $vps2^{PP6}$ / TM6B
Fig. 3G,G'	*hs-flp*;; FRT82B, *ubi-gfp* × FRT82B, $Ubpy^{KO}$, $vps2^{PP6}$/ TM6B
Fig. 4	*hs-flp*; *arm-lacZ,* FRT40A × hrs^{D28}, FRT40A / Gla, Bc
Fig. S1A,G	*ap*-Gal4, UAS-*mCD8-gfp* / CyO × 5798R-1 / TM3
Fig. S1B-E,I-J	*ap*-Gal4, UAS-*mCD8-gfp* / CyO × VDRC #107623
Fig. S1F,H, Fig. S3	*ap*-Gal4, UAS-*mCD8-gfp* / CyO × 5798R-2 / SM1
Fig. S1K,M	*ap*-Gal4, *dpp-lacZ* / CyO × VDRC #107623 at 29°C
Fig. S1L,N	*ap*-Gal4, *ptc-lacZ* / CyO × VDRC #107623 at 29°C
Fig. S2J-O, Fig. S6	*hs-flp*; *ubi-gfp,* FRT40A × hrs^{D28}, FRT40A / Gla, Bc
Fig. S4G-G'"	*MS1096*-Gal4, UAS-*mCD8-gfp* × VDRC #107623
Fig. S4H-H'"	*MS1096*-Gal4, UAS-*mCD8-gfp*; UAS-

	DTS5 / + × VDRC #107623 at 29°C
Fig. S4I-I’”	*MS1096*-Gal4, UAS-*mCD8-gfp* × VDRC #38821
Fig. S4J-J’”	*MS1096*-Gal4, UAS-*mCD8-gfp*;; VDRC #38821 / + × VDRC #107623
Fig. S7A-A’”	*MS1096*-Gal4, UAS-*mCD8-gfp* × TRiP #28026
Fig. S7B-B’”	*MS1096*-Gal4, UAS-*mCD8-gfp* × UAS-*FLAG-Ubpy*
Fig. S7C-C’”	*MS1096*-Gal4, UAS-*mCD8-gfp*;; TRiP #28026 / + × UAS-*FLAG-Ubpy*
Fig. S7D-E”’	*hs-flp*, *tub*-Gal4, UAS-*mCD8-gfp*; *tub*-Gal80, FRT40A × hrs^{D28}, FRT40A / +; UAS-*FLAG-Ubpy* / +
Fig. S8A-F	*ap*-Gal4, UAS-*mCD8-gfp* / CyO; *tub*-Gal80ts × VDRC #107623

Zhang et al. Figure S1

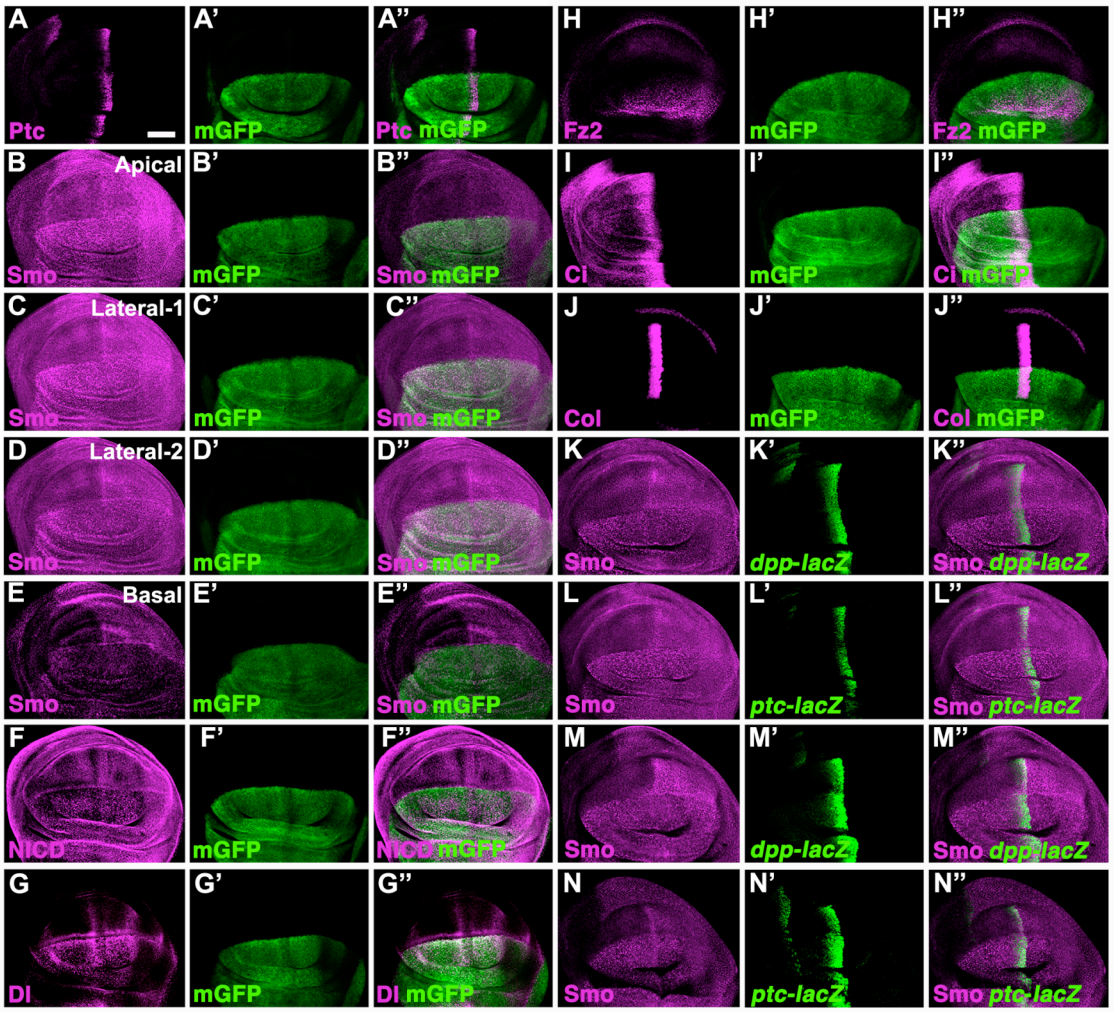

Figure S1. *Ubpy* RNAi results in mis-localization of membrane signaling proteins in the wing disc.

(A) Ptc is accumulated in punctate structures in *Ubpy* RNAi-expressing cells that are marked by a membrane-localized mCD8-GFP (mGFP). The *ap-Gal4* driver confers transgenic RNAi expression in the dorsal compartment of the wing disc, leaving the ventral region, which is composed of wildtype cells, as the internal control. Note that the localization of GFP at the plasma membrane is not affected in *Ubpy* RNAi cells, which serves as an additional negative control.

(B-E) Distribution of Smo-containing vesicles in the wing disc is examined in different focal planes along the *Z*-axis. In *Ubpy* RNAi expressing cells, Smo accumulation is evident in apical (B) and lateral (C, D) focal planes. The reported down-regulation of Smo is only observed at the basal-most focal plane in the posterior compartment (E).

(F-H) Similar localization defects are observed for N (F), Dl (G) and Fz2 (H) in the wing disc. Mukai et al. (2010) reported that ectopically overexpressed FLAG-Fz2 protein is down-regulated in *Ubpy* RNAi expressing cells. We found that endogenous Fz2 protein is accumulated when the same condition was applied.

(I-L) Hh signaling activity is not obviously altered in *Ubpy* RNAi expressing cells, as indicated by normal expression patterns of Ci (I) and Col (J) protein as well as *dpp-lacZ* (K) and *ptc-lacZ* (L) reporters. Note that expansion of *dpp-lacZ* (M) and *ptc-lacZ* (N) is observed in a small percentage of *Ubpy* RNAi wing discs when fly crosses are maintained at 29ºC. Scale bar: 50 μm.

Zhang et al. Figure S2

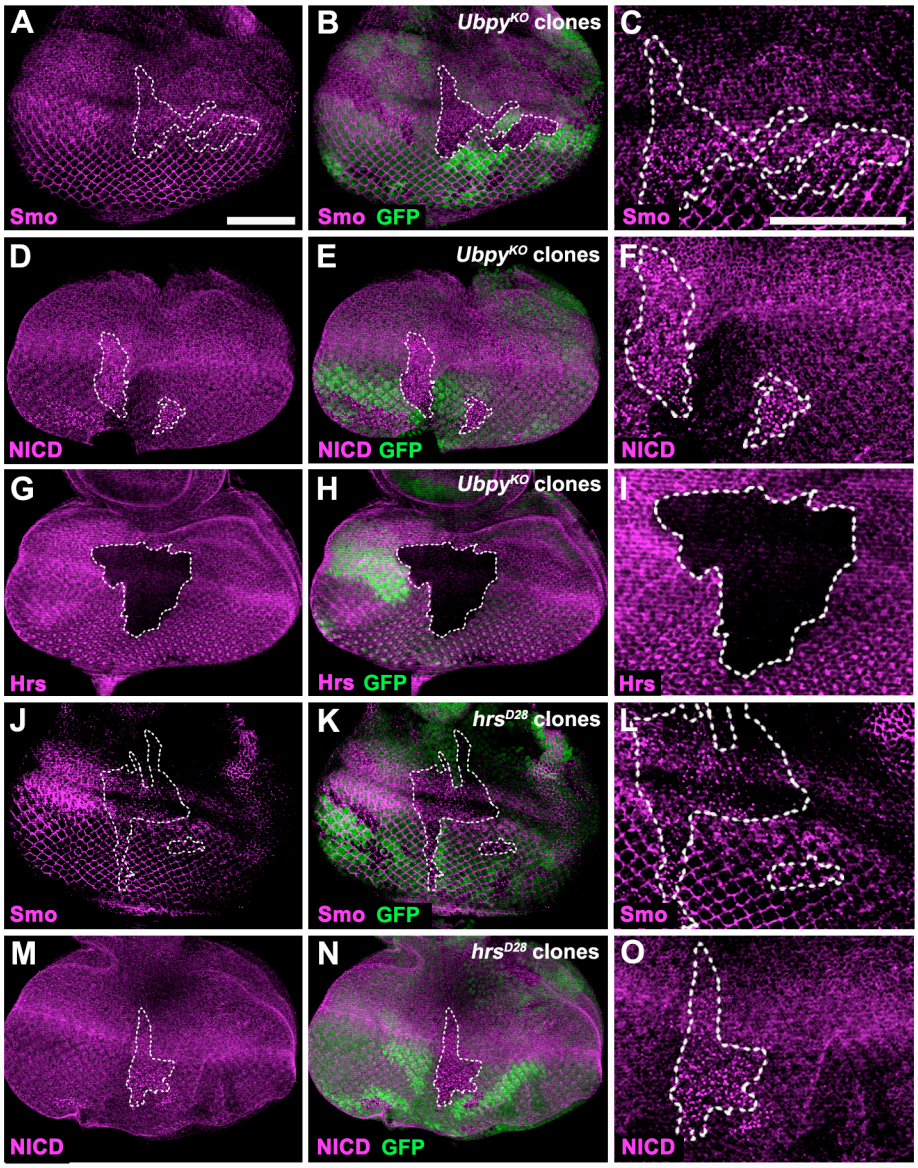

Figure S2. *Ubpy* and *Hrs* regulate localization of signaling proteins in the eye disc. In agreement with the wing disc results, loss of *Ubpy* leads to accumulation of Smo (A) and N (D), and degradation of Hrs (G) in the eye disc. Smo (J) and N (M) are mis-localized in hrs^{D28} mutant clone cells in the eye disc. Somatic clones are circled by dashed lines. Higher magnification images of marked clones are shown (C, F, I, L, O). Scale bar: 50 μm.

Zhang et al. Figure S3

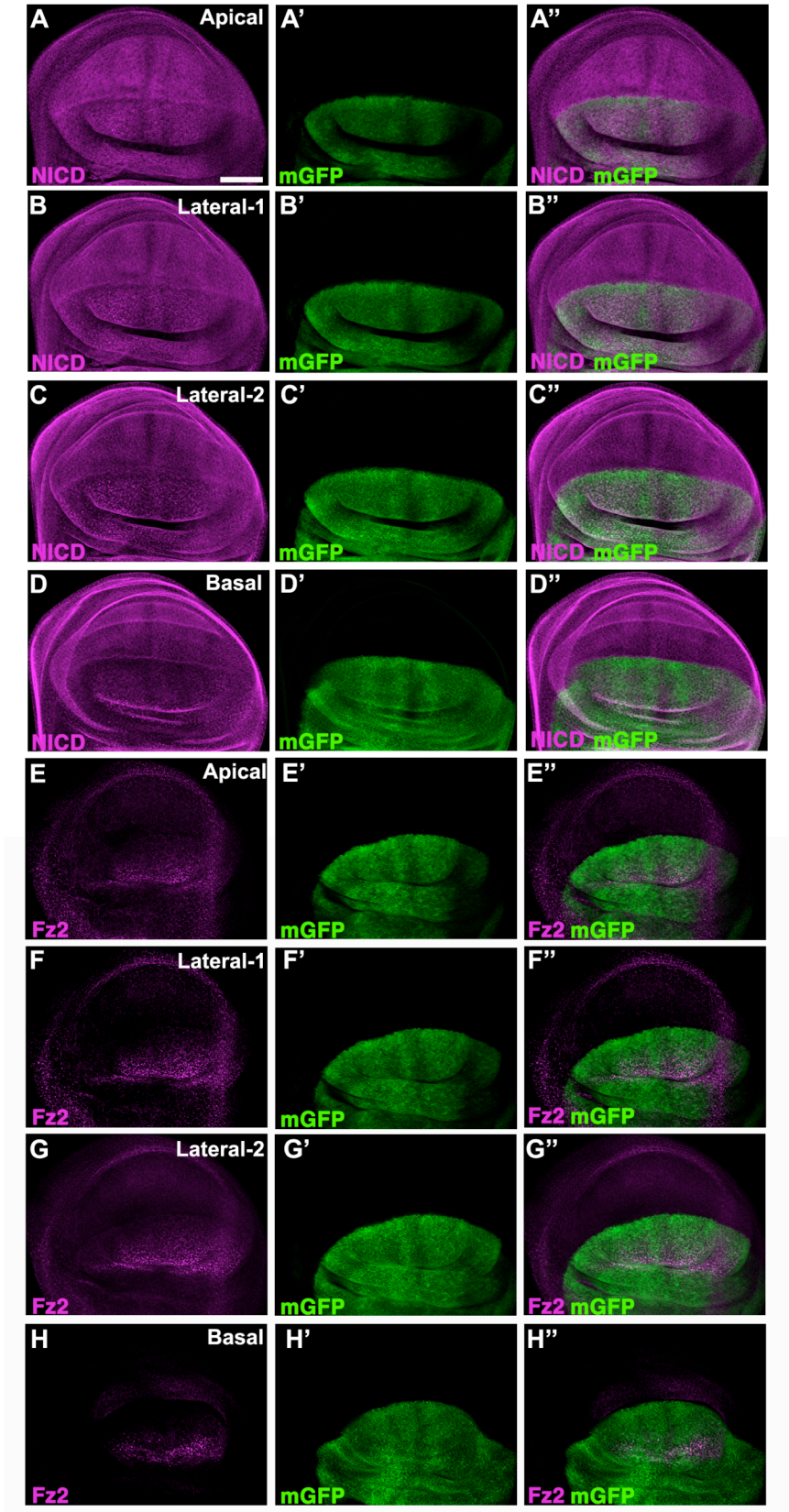

Figure S3. *Ubpy* RNAi results in mis-localization of Notch and Fz2 expression in the wing disc.

Ubpy RNAi is expressed in the dorsal compartment of the wing disc that is marked by a membrane-localized mCD8-GFP (A'-H'). Distribution of Notch (NICD)- (A-D) and Fz2- (E-H) containing vesicles in the wing disc is examined in different focal planes along the Z-axis. Unlike polarized Smo accumulation, heightened Notch and Fz2 expression are observed in all membrane domains. Scale bar: 50 μm.

Zhang et al. Figure S4

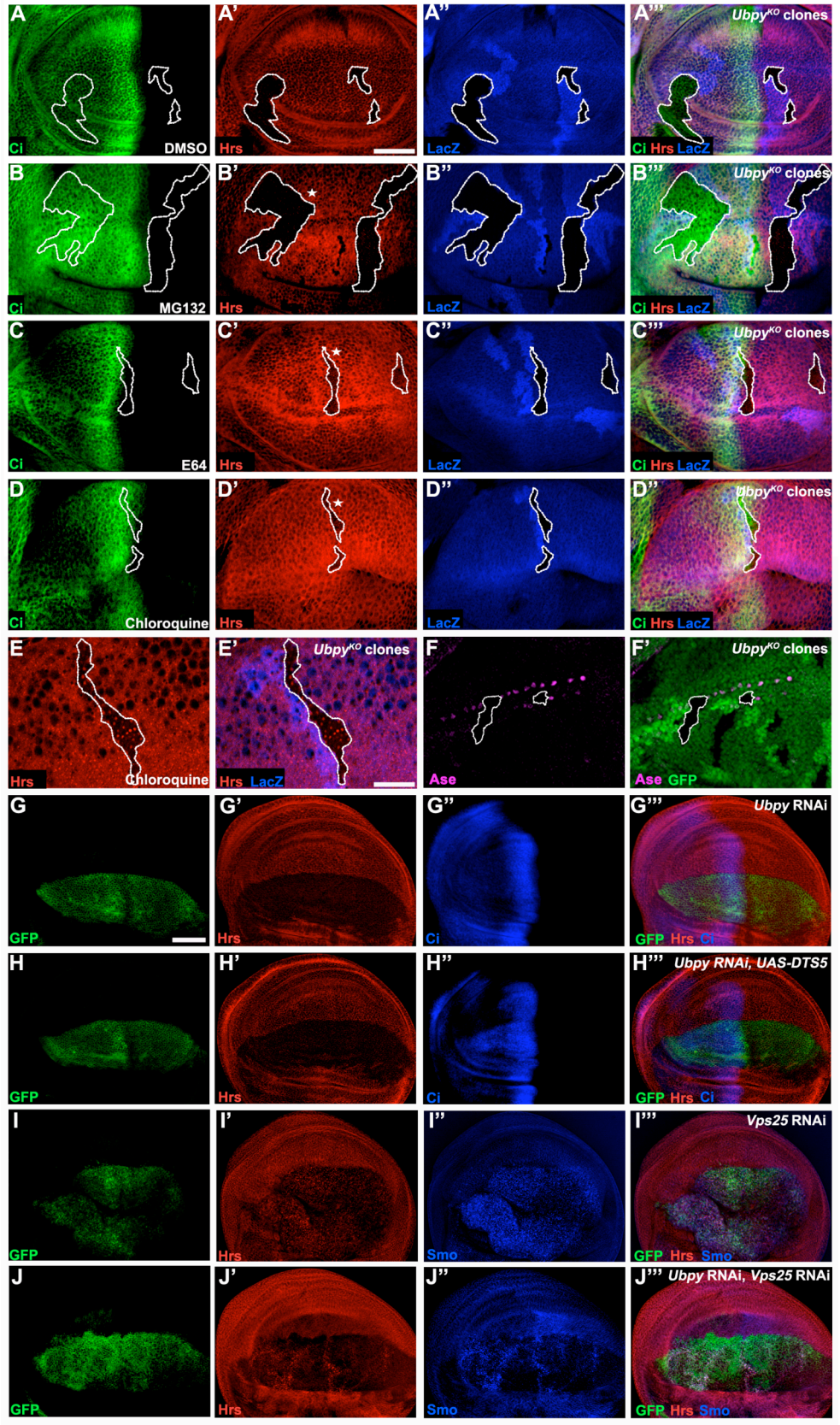

Figure S4. Disruption of lysosomal function prevents Hrs from degradation.

(A-E) Wing discs bearing *Ubpy*^{KO} clones (marked by lack of LacZ) are mock treated with DMSO (A), incubated with MG132 (B) to inhibit proteasome function, E64 (C) and chloroquine (D) to inhibit lysosome activity. Hrs is degraded in *Ubpy* clones (A'). Disrupting lysosome function rescues Hrs from degradation (C'-E'), whilst inhibiting proteasome function has no effect (B'). Higher magnification images of clones marked with asterisk marks in panels B-D are shown in Fig. 3B, 3C and Fig. S4E, respectively. Note that similar effect of *Ubpy*^{KO} on Hrs is observed regardless of the clone location in wing discs (A-D).

(F and F') Ase staining along the presumptive wing margin is abolished in *Ubpy*^{KO} clones (marked by lack of GFP), suggesting that Wg signaling is compromised.

(G-J'") *Ubpy* RNAi overexpressed in the dorsal compartment of the wing disc (G) results in downregulation of Hrs (G'). Disrupting 20S proteasome core component b6 (Pros26) activity by a dominant-negative *DTS5* mutant fails to rescue *Ubpy* RNAi-mediated Hrs degradation. Note that the abundance of Hh signaling transcription factor Ci, which is subject to proteasomal degradation (Du et al., 2011), is increased (H"). In contrast, *Ubpy* RNAi-mediated Hrs degradation is rescued when the expression of *Vps25*, an ESCRT-II complex member, is reduced by RNAi (J'). Somatic clones are circled by dashed lines. Scale bar: 50 μm (A-D", F-J'") and 20 μm (E and E').

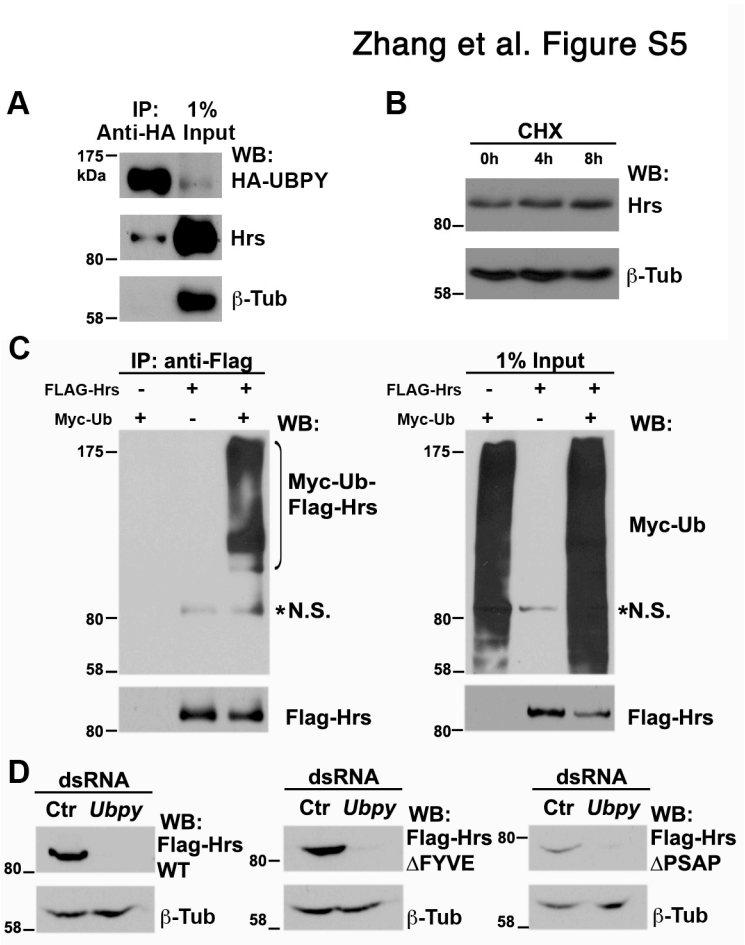
Zhang et al. Figure S5
A
IP: Anti-HA
1% Input
175 kDa
WB: HA-UBPY
Hrs
80
β-Tub
58
B
CHX
0h
4h
8h
WB:
Hrs
80
β-Tub
58
C
IP: anti-Flag
1% Input
FLAG-Hrs - + +
Myc-Ub + - +
WB:
175
Myc-Ub-Flag-Hrs
*N.S.
80
58
Flag-Hrs
Myc-Ub
D
dsRNA
Ctr Ubpy
WB:
Flag-Hrs WT
Flag-Hrs ΔFYVE
Flag-Hrs ΔPSAP
β-Tub

Figure S5. Ubpy regulates Hrs stability *in vitro*.

(A) Ubpy co-immunoprecipitates with endogenous Hrs in S2 cells.

(B) In the presence of physiological level of Ubpy, endogenous Hrs is stable for indicated hours upon treating S2 cells with cychloheximide (CHX), an inhibitor for nascent protein synthesis. β-Tubulin serves as the loading control**.**

(C) Protein lysates from S2 cells overexproducing either FLAG-Hrs, Myc-Ub alone or both proteins together are immunoprecipitated with anti-FLAG gel followed by immunoblotting with antibodies for Myc and FLAG tags, respectively. This experiment serves as a control for that shown in Fig. 3H.

(D) *Ubpy* dsRNA treatment in S2 cells leads to degradation of wildtype Hrs and mutant forms of Hrs lacking either the FYVE motif (for membrane association) or the PSAP domain (for ESCRT-I interaction), respectively. β-Tubulin serves as the loading control.

Zhang et al. Figure S6

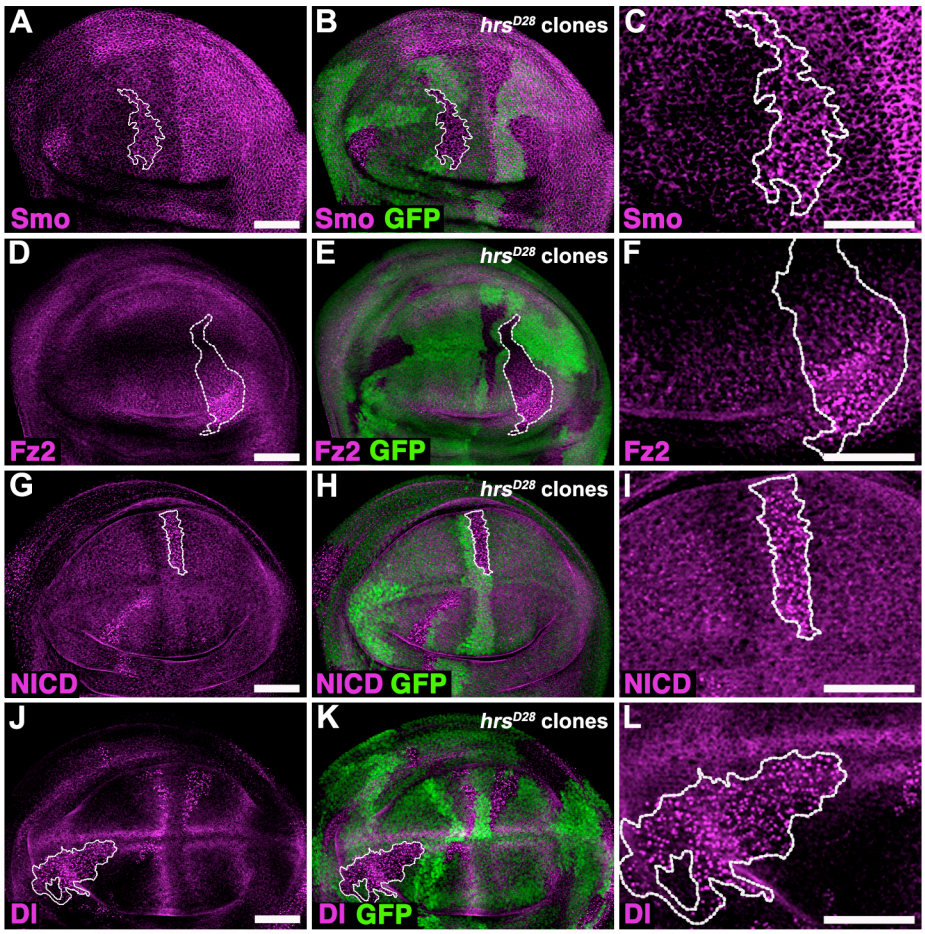

Figure S6. *Hrs* regulates subcellular localization of membrane signaling proteins in the wing disc.

Multiple membrane signaling proteins, including Smo (A), Fz2 (D), N (G) and Dl (J) are accumulated as punctate structures in hrs^{D28} mutant clone cells in wing discs. Higher magnification images of marked clones are shown (C, F, I, and L). Note that Smo accumulation is found at apical membrane domains in hrs^{D28} mutant clone cells. Somatic clones are circled by dashed lines. Scale bar: 50 μm.

Zhang et al. Figure S7

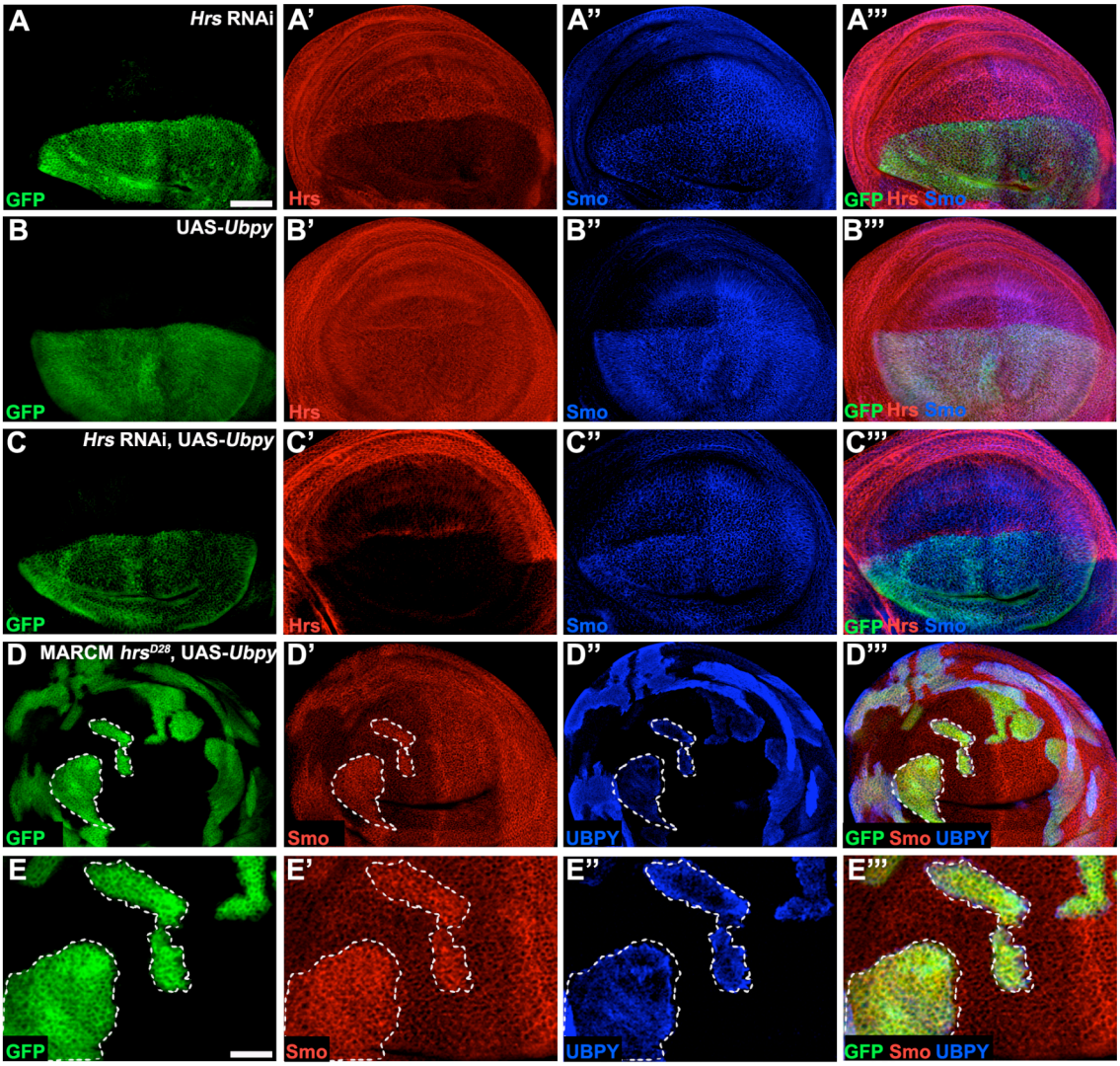

Figure S7. The effect of ectopic *Ubpy* activity on Hrs and Smo protein.

(A-C'") *Hrs* dsRNA expression in the dorsal compartment of the wing disc (marked by GFP) results in apical accumulation of Smo in enlarged vesicles (A"). In contrast, overexpressing UAS-*FLAG-Ubpy* stabilizes Smo protein but does not alter its subcellular localization (B"). When both *Hrs* dsRNA and UAS-*FLAG-Ubpy* are overexpressed, stabilization of Smo protein is observed (C"), a phenotype similar to that caused by ectopic *Ubpy* activity.

(D-E'") UAS-*FLAG-Ubpy* is expressed in hrs^{D28} MARCM clones (D-D'"). Higher magnification images are shown (E-E'"). Stabilization of Smo, is observed (D'). However, Smo subcellular localization is not altered. This result suggests that Ubpy activity is sufficient to stabilize Smo, which might be distinct from its ability to control Smo localization. Somatic clones are circled by dashed lines. Scale bar: 50 μm.

Zhang et al. Figure S8

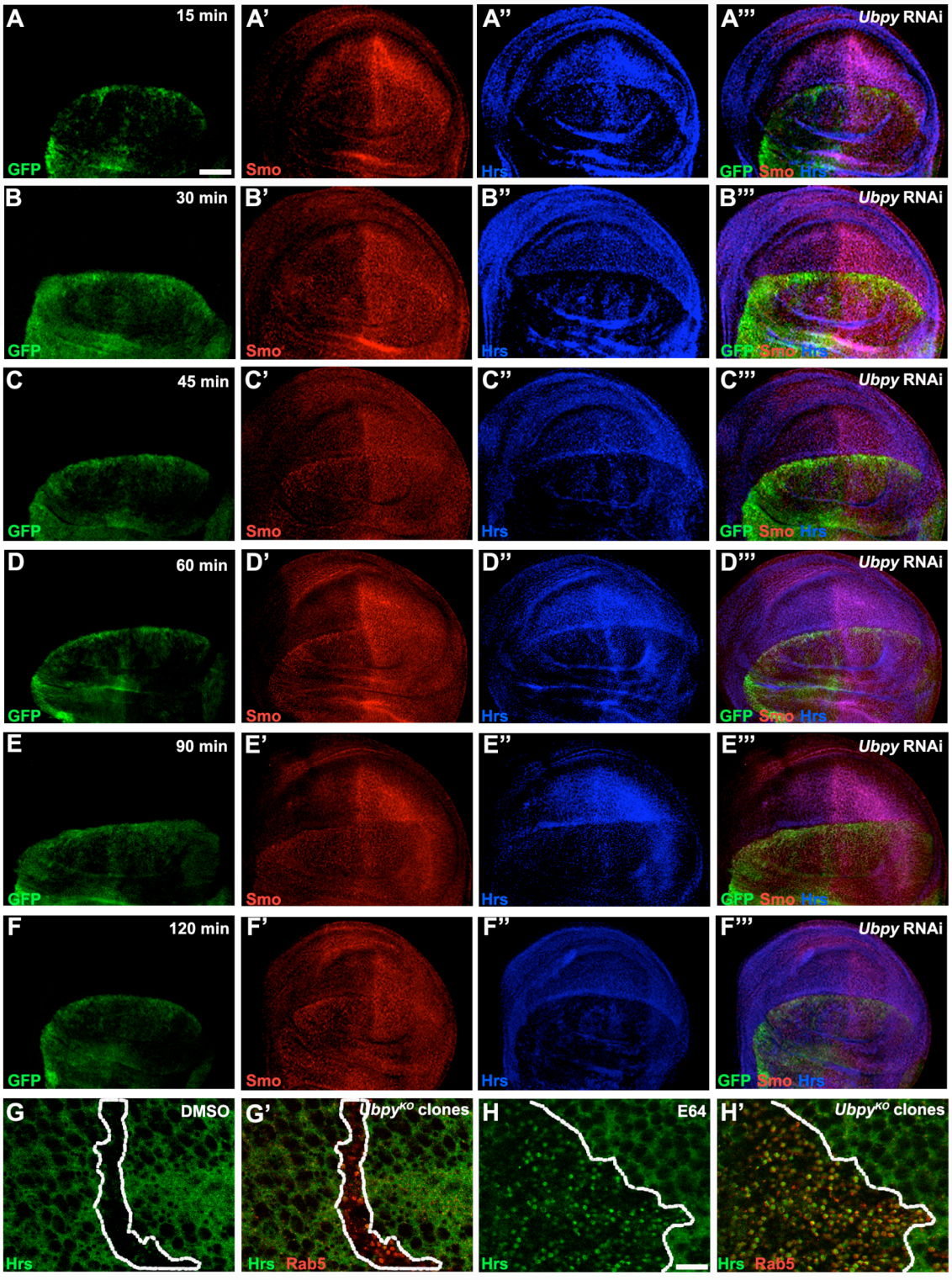

Figure S8. The relationship between Hrs degradation and Smo accumulation in enlarged vesicles.

(A-F'") Time course analyses of the *Ubpy* RNAi effect on Hrs degradation and Smo accumulation. UAS-*Ubpy* dsRNA transgene expression is controlled by a temperature-sensitive Gal80 (Gal80ts). *Ubpy* dsRNA is not expressed at room temperature. Upon shifting third-instar larvae to 29ºC for 30 minutes (pulse), Gal80ts is no longer able to inhibit Gal4 activity, thus allowing the expression of *Ubpy* dsRNA. Fly larvae are then moved back to room temperature (chase) for different length of time as shown. Hrs is readily degraded as early as 15 minutes of chase. However, obvious Smo accumulation in enlarged vesicles is only observed after 45 minutes of chase.

(G-H) In $Ubpy^{KO}$ clones, disrupting lysosome function by E64 prevents Hrs degradation (H), which co-localizes with Rab5 (H'). Somatic clones are circled by dashed lines. Scale bar: 50 μm (A-F) and 20 μm (G-H).